Desalination and Water Treatment
www.deswater.com

doi: 10.5004/dwt.2022.28522

261 (2022) 42–56
June

Modification and operational stability evaluation of a miniaturized reciprocating-switcher energy recovery device for SWRO desalination system

Hui Zhang[a,b,c], Yue Wang[a,b,c,*], Zheng Sun[a,b,c], Jiaqi Guo[a,b,c], Jun Li[a,b,c], Shichang Xu[a,c]

[a]*Chemical Engineering Research Center, School of Chemical Engineering and Technology, Tianjin University, Tianjin 300072, China, emails: tdwy75@tju.edu.cn (Y. Wang), zhang_hui_96@163.com (H. Zhang), tdsz@tju.edu.cn (Z. Sun), gjq17627810617@163.com (J. Guo), 18302212086@163.com (J. Li), xushichang@sina.com (S. Xu)*
[b]*State Key Laboratory of Chemical Engineering, Tianjin 300072, China*
[c]*Tianjin Key Laboratory of Membrane Science and Desalination Technology, Tianjin 300072, China*

Received 6 November 2021; Accepted 17 April 2022

ABSTRACT

The self-boosting energy recovery device (SB-ERD) integrated with the booster pump function can reduce the power consumption of small and medium-sized seawater desalination systems. Nevertheless, for SB-ERD, the flow rate and pressure pulsation of HP brine and nonadjustable capacity are presented in the operation process, affecting its further application in seawater reverse osmosis (SWRO) systems. In this paper, the SB-ERD was modified to a miniaturized reciprocating-switcher energy recovery device (MRS-ERD). Then a SWRO experimental test platform equipped with MRS-ERD was built to evaluate operational performance. The experimental results show that the pressure pulsation amplitude of HP brine is maintained at 0.20 MPa, and the flow rate pulsation amplitude is kept only between 0.153 and 0.186 m^3/h. At design capacity, the pressure pulsation ratio of HP brine is reduced by 2.41% compared with SB-ERD, and the flow rate pulsation ratio is only 1.5%, which is 4.05% lower than that of SB-ERD, revealing excellent operational stability. Furthermore, under 5.0 MPa and 80%–130% of the design capacity (12 m^3/h), the MRS-ERD can run with a constant efficiency above 96.33% and a leakage ratio of 1.3%–2.7%, which is competitive in commercial products. Hence, MRS-ERD exhibits huge application prospects in small and medium-sized SWRO systems.

Keywords: Seawater reverse osmosis; Energy recovery device; Pulsation; Operation stability; Energy efficiency

1. Introduction

The scarcity of freshwater resources has become the second-largest world environmental problem after global warming and will also be another resource crisis following the oil resource crisis [1]. Since seawater resources account for about 97% of the total water resources of the earth, seawater desalination has developed an effective way to solve the problem of the shortage of freshwater resources [2,3]. Seawater reverse osmosis (SWRO) stands out from many desalination technologies for advantages of low power consumption, simple operation, high efficiency, and so on [4–6]. However, in the early stage of seawater reverse osmosis technology development, its practical application was limited because of high energy consumption and operation cost [2,7,8]. The emergence of energy recovery devices (ERDs) reversed this pattern. ERD can significantly save energy by recovering the residual pressure of high-pressure

* Corresponding author.

brine and delivering the pressure energy back to feeding seawater [4–6,9].

As the mainstream ERDs on the market, isobaric ERDs are separated into two categories: rotary type and valve-controlled type [10–13]. Rotary ERDs have the advantages of high energy recovery efficiency, compact device structure, and small footprint. The main representative product of the rotary ERD is the PX. The core components of the PX are mainly composed of a ceramic rotor, a pair of ceramic end caps and a ceramic sleeve on the outside of the rotor [14]. The areas of the high-pressure zone and the low-pressure area remain constant, ensuring the stable operation of the PX device. The valve-controlled ERDs occupies an important market position with convenient operation and maintenance, low technical threshold, and high energy recovery efficiency. The main representative product of valve-controlled ERDs is DWEER. DWEER comprises three parts: switcher, hydraulic cylinders, and check valve group [11]. The switcher (Linx valve), as the vital component of the energy recovery device, controls the regular entry and exit of HP and LP fluid into and out of the hydraulic cylinder. The hydraulic cylinder is the primary place for pressure exchange. The check valve group is used as a passive actuator to cooperate with the switcher to complete LP and HP fluids in and out of the hydraulic cylinder. Many pieces of research have been done on the development and study of valve-controlled energy recovery devices [15–19]. Zhou et al. [20] built a SWRO desalination experiment platform and conducted a capacity flexibility test on RS-ERD. Sun et al. [21] have developed a three-cylinder energy recovery device (TC-ERD) that matched the control logic and tested the operational stability on the SWRO desalination experiment platform. The research of valve-controlled energy recovery devices tends to be large-scale, but the research of small and medium-sized devices is imperfect. In the field of small and medium-sized seawater desalination, the iSave series products of Danfoss in Denmark couple the energy recovery device, booster pump and motor together to realize the integration of pressure energy recovery and booster functions, with a high degree of integration [22]. SALINO Pressure Center integrates energy recovery device, booster pump, motor and high-pressure pump [23]. This 4-in-one integrated device can meet the process requirements of small and medium-sized seawater desalination systems. However, the integrated design reduces the floor space and also causes problems such as complicated device structure and difficult maintenance.

Currently, most small and medium-sized seawater desalination platforms are not equipped with energy recovery devices due to the high price, high water quality requirements, and maintenance difficulties of rotary energy recovery devices, resulting in increased energy consumption and low-cost performance. As one of the critical technologies for SWRO, energy recovery technology can save about 50% energy consumption by recovering the residual pressure energy of HP concentrated brine [24]. The valve-controlled energy recovery device has the advantages of convenient operation and maintenance, low technical threshold. However, few small and valve-controlled type ERDs can be applied to medium-sized seawater desalination platforms. Tian et al. [25] developed a self-boosting energy recovery device and conducted an experimental evaluation on the SWRO system, in which the pulsation of pressure and flow rate affect the operation stability of the SB-ERD, and the unregulated flow rate affects the further application in seawater reverse osmosis systems. To solve the above application problems, it is necessary to develop a miniaturized valve-controlled energy recovery device. Although the ERDs can effectively recover the pressure energy from the HP brine, greatly reducing the energy loss in the seawater desalination process, the impact on the seawater desalination systems during its operation cannot be ignored [26,27]. In particular, the stability of pressure and flow rate is directly related to the separation performance of the membrane module [28–30], so it is particularly essential to study the operation stability of the ERD.

In this paper, the SB-ERD was modified to a miniaturized reciprocating-switcher energy recovery device (MRS-ERD). A seawater desalination test platform coupled with a miniaturized reciprocating-switcher energy recovery device was established to evaluate an operational stability and performance. The pressure, flow rate and pressure loss fluctuations of HP and LP fluid were studied to evaluate the operational stability of ERD. MRS-ERD was equipped with a HP overlap function to alleviate the pulsation of the pressure and flow rate of the HP fluid. The leakage and energy recovery efficiency of the MRS-ERD under different capacities were investigated to evaluate operational performance. Hence, this paper aims to improve the operational stability by reforming the SB-ERD and lay a theoretical foundation for the commercial application of MRS-ERD.

2. Experiments

2.1. Staple components of MRS-ERD

As shown in Fig. 1, MRS-ERD has made two changes on the basis of SB-ERD. (1) Two one-way throttle valves are added to the hydraulic actuator to precisely control the inflow speed of the driving fluid, thereby controlling the reversing speed of the switcher, reducing fluid pulsation and improving the device operation stability. (2) The MRS-ERD is removed the piston rod and used a pipeline-type booster pump. The pipeline booster pump is integrated in the pipeline, which greatly reduces the floor space.

The miniaturized reciprocating-switcher energy recovery device is an isobaric valve-controlled ERD composed of three parts: a passive check valve nest, a fluid switcher, and two hydraulic cylinders. Besides, a high-pressure fluid stream is led from the HP brine to drive the hydraulic switcher. A regulator is set to regulate the driving fluid. Two two-position three-way solenoid valves are connected to control the HP brine to enter the fluid switcher alternately. Among them, the fluid switcher is the core component of the energy recovery device. It establishes a high-pressure channel and guides HP brine into a hydraulic cylinder to participate in the pressurization process, establishes a low-pressure channel, and guides the LP brine to be discharged from another hydraulic cylinder to complete the pressure relief process.

The fluid switcher is essentially a two-position five-way valve. Fig. 2 is a cross-sectional view of the fluid

switcher in the forward and backward positions. A hydraulic actuator is the driving structure of the fluid switcher. The switcher can cyclically reciprocate in two working positions (forward position and backward position) [25]. As the fluid switcher is in a forward working position, as presented in Fig. 2b, the HP valve plate 1 and the LP valve plate 1 are closed, and the HP valve plate 2 and the LP valve plate 2 are opened. At this time, the HP brine interface and the hydraulic cylinder interface 1 are connected to create a high-pressure channel, and LP brine interface 2 and the hydraulic cylinder interface 2 are connected to frame a low-pressure channel. As shown in Fig. 2c, when the fluid switcher is in a backward working position, the high-pressure valve plate 1 and the LP valve plate 1 are opened, and the HP valve plate 2 and the LP valve plate 2 are closed. At the moment, the HP brine interface and the hydraulic cylinder interface 2 are connected to build a high-pressure channel, and LP brine interface 1 and hydraulic cylinder interface 1 are connected to establish a low-pressure channel. The time control mode is adopted to realize the orderly switching of the fluid switcher. In order to avoid the HP brine pressure rise caused by the complete closing of the high-pressure channel, it should be ensured that before one HP valve plate is closed, the other HP valve plate has been opened [31]. In other words, the HP overlap function is set to decrease the pressure fluctuation of HP fluid. The HP overlap time of MRS-ERD is longer than SB-ERD but still less than one second.

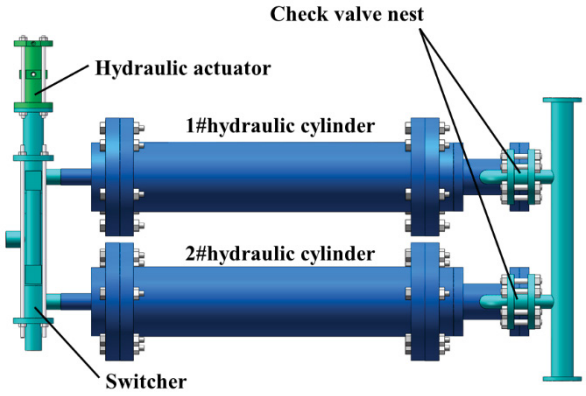

Fig. 1. Main components of ERD.

2.2. SWRO desalination experimental platform

A SWRO desalination test platform was built to evaluate the operational performance of the energy recovery device. The SWRO desalination experiment platform mainly includes the following devices: feed pump, HP pump, booster pump, large flux filter, reverse osmosis membrane module, data acquisition, and control system. Fig. 3 shows the flow chart of the SWRO desalination experiment platform, and Fig. S1 the field diagram of the SWRO system equipped with MRS-ERD is included in the supporting literature. The main technical components are shown in Table 1.

Tap water and sea salt were used to configure feed seawater, and the salinity of feed seawater (mass fraction of NaCl) is about 3.6%. The feed pump increases the pressure of the seawater, and one part of feed seawater is supplied to the HP pump, which raises the seawater's pressure to reach the inlet pressure of the reverse osmosis membrane. The other part is supplied to the energy recovery device. The seawater can be divided into two streams of HP brine

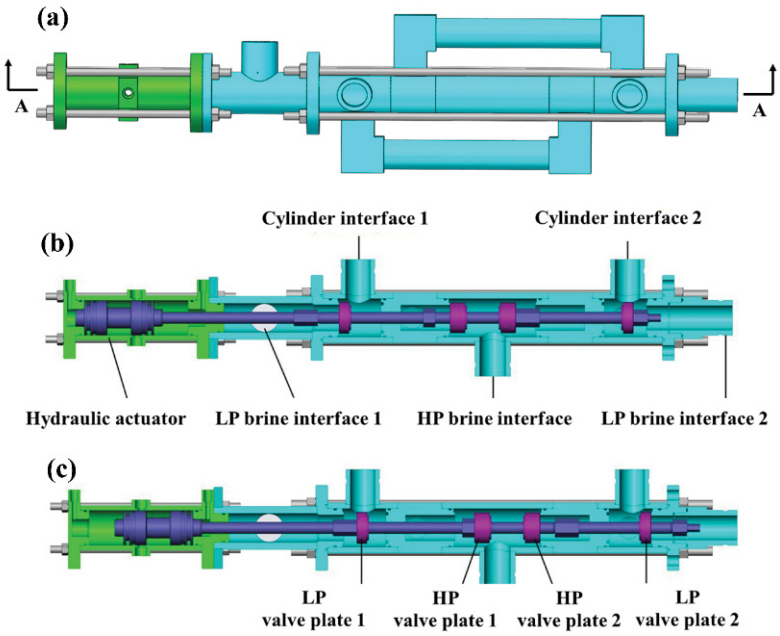

Fig. 2. (a) Three-dimensional modeling of the fluid switcher, (b) cross-sectional view of plane A-A at forward position and (c) the cross-sectional view of plane A-A at backward position.

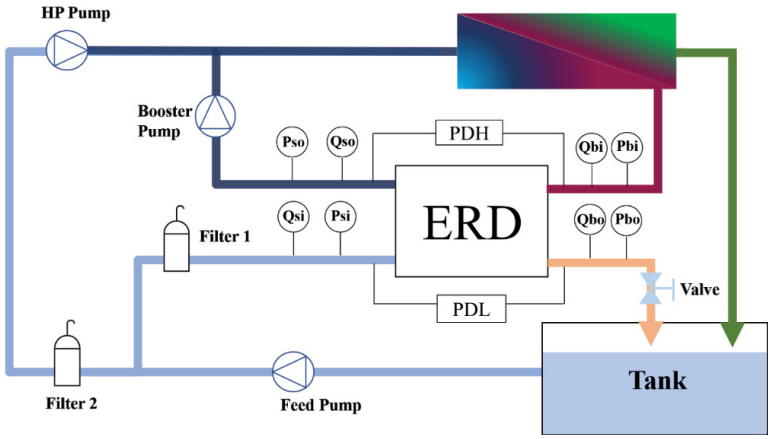

Fig. 3. Flow chart of SWRO test platform.

Table 1
The technical parameters of main parts

Parts	Technical parameters	Manufacturer
Feed pump	20 m^3/h@58 m	CNP
HP pump	APP7.2	DANFOSS
Booster pump	18 m^3/h@40 m	GRUNDFOS
Membrane element	Salt rejection: 99.7%	VONTRON
Membrane housing	1,000 psi	ROPV
Filter 1 & 2	5 μm	FUNITER & BAONA

and permeate water through the reverse osmosis membrane. The HP brine enters the energy recovery device and exchanges pressure with the LP seawater. A booster pump pressurizes the HP seawater from the energy recovery device unit to reach the inlet pressure of the reverse osmosis membrane. The HP seawater and the outlet fluid of the HP pump enter the reverse osmosis membrane together after being combined. The permeate water is returned to the original water tank to keep the seawater's salinity constant.

The data acquisition and control system are mainly composed of two two-position three-way valves, an industrial personal computer (IPC) (Advantech, IPC-610), and two programmable logic controllers (PLCs) (Siemens, S7-200CN). The experimental operation and data acquisition of the seawater desalination system is carried out on the industrial computer. The control instructions are sent to two programmable logic controllers through the industrial computer. ERD-PLC is used to control the energy recovery device, and SWRO-PLC controls the reverse osmosis desalination system. ERD-PLC adopts the time control method and sends the reversing instruction to the solenoid valve through the preset control interval (20 s) to realize the orderly switching and ensure the pressure boost and pressure relief process. SWRO-PLC controls the start and stop of the pump in the system and completes the data collection of pressure, flow rate and pressure loss. The data accuracy of pressure and flow rate is ± 0.5%, and the measurement accuracy of pressure loss is ± 0.5%. The sampling period of SWRO-PLC is 1 s.

3. Results and discussions

By setting the same operating pressure (5.0 MPa) and different processing capacity gradient operation mode, the characteristics of pressure, flow rate, and pressure loss of HP and LP fluids with the change of processing capacity were explored. And the leakage situation and energy recovery efficiency of the ERD are evaluated. Six testing conditions are adopted to evaluate the performance of the device. When discussing the pulsation of flow rate and pressure, we selected four typical flow rate test conditions near the design flow rate (12 m^3/h) for discussion. Since the pulsation of the fluid is basically the same under the two lower flow conditions (6 and 8 m^3/h), considering that the fluid pulsation is smaller at low flow rate, the pressure and flow pulsation performance of the MRS-ERD is not discussed. Figs. S2–S7 for flow rate and pressure and pressure loss at lower flow rate conditions (6 and 8 m^3/h) have been supplemented to the supporting literature. In the discussion of the leakage and efficiency performance of the device, the six test conditions of flow rate were selected, taking into account the flexibility of device capacity.

3.1. Fluctuation characteristics of HP fluid for MRS-ERD

In the SWRO desalination process, the HP fluid must maintain a high pressure to ensure the normal water production process. Maintaining the stability of the HP fluid is conducive to reducing the impact of the shock force

caused by pressure fluctuations. It is of great significance to the stable operation of the SWRO system. In this part, the operation stability of the MRS-ERD was conducted in terms of the pulsation amplitude of HP fluid. The pulsation amplitude is determined by the difference between the mean values of the maximum value (peak) and minimum value (trough). The pressure pulsation ratio is the ratio of pressure pulsation amplitude to operating pressure, and the flow rate pulsation ratio is the ratio of flow rate pulsation amplitude to processing capacity. MRS-ERD adopts the isobaric working principle. HP brine directly pressurizes HP seawater to realize pressure exchange. Therefore, HP seawater and HP brine have the same fluid characteristics, and HP brine is chosen as the evaluation index in this section. The design capacity of MRS-ERD is 12 m^3/h.

3.1.1. Pressure fluctuation of HP brine in different capacities

Fig. 4 is the HP brine's pressure curve with ERD capacity from 10 to 16 m^3/h. The ERD adopts a time control mode, and the cycle time under standard conditions is 20 s. As shown in Fig. 4, at 5.0 MPa operating pressure, HP brine cyclical pressure fluctuations downwardly and has little change in the characteristics of amplitude fluctuation. When the operating pressure is 5.0 MPa, the capacity varying from 10 to 16 m^3/h, the pulsation amplitude of the HP brine is maintained at substantially 0.20 MPa (about 4.0% pulsation ratio), which is about 2.5% lower than that of SB-ERD. Because the ERD has the HP overlap function to ensure the continuity of the HP brine, further the reduction of the HP brine pressure pulsation change is brought about [31,32].

In SB-ERD, the pressure fluctuation of the HP brine is caused by the inertia of the HP fluid and the piston moving [25]. In MRS-ERD, the downward fluctuation of HP brine pressure is mainly caused by the diversion effect of the hydraulic actuator. Since the hydraulic actuator needs to be driven by a divided flow rate during the transposition process, it requires HP brine pressure, HP brine flow rate, and permeate flow rate to compensate for a difference. The pressure of HP brine is the most sensitive to the diversion

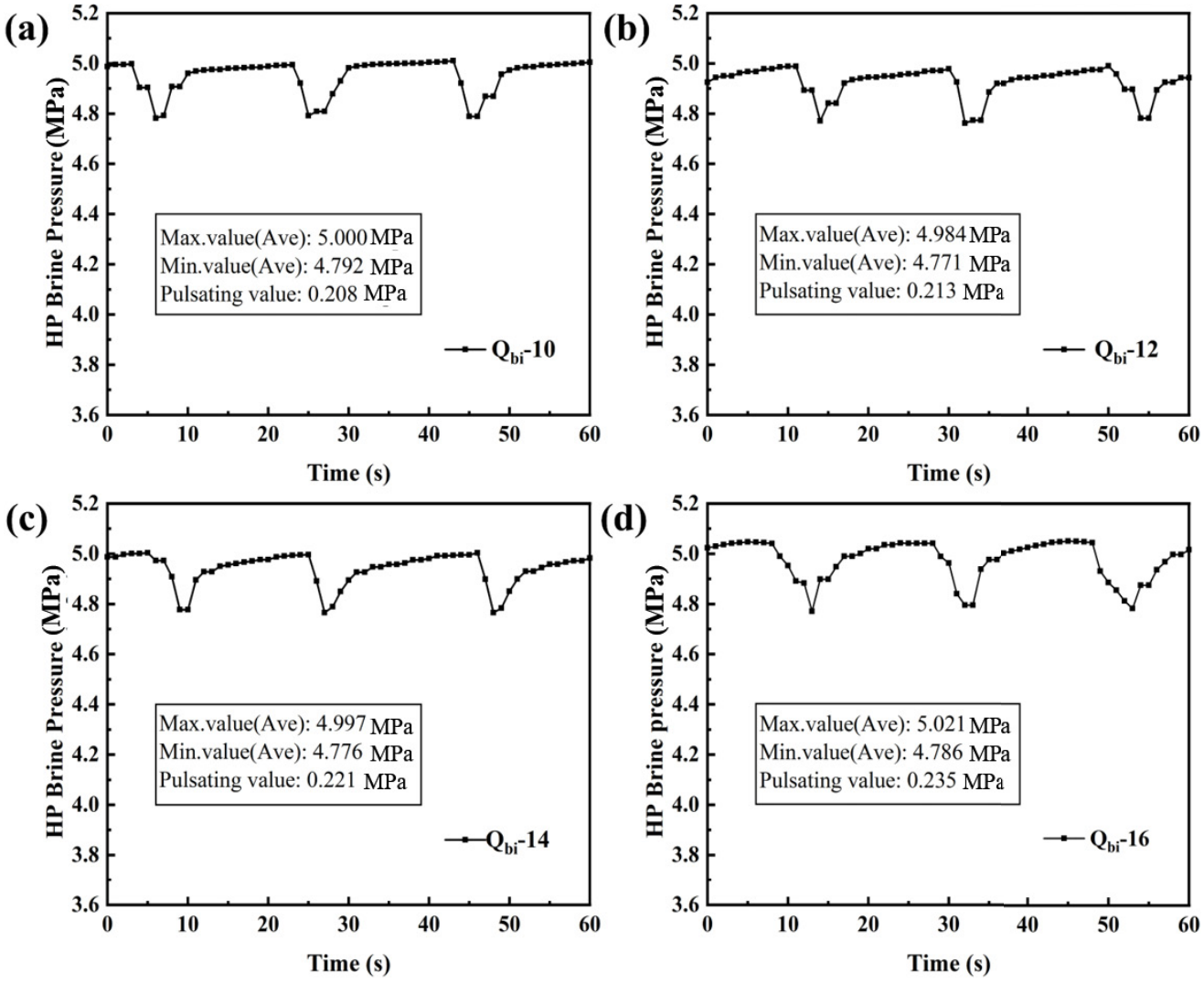

Fig. 4. Pressure curve of the HP brine at different capacities.

effect of the hydraulic actuator. As shown in Figs. 4 and 5, the pressure change precedes the flow rate change in time. HP brine pressure is the first compensation amount for the split flow of the hydraulic actuator. When the hydraulic actuator is switched, the flow area of the HP brine increases. But in fact, the flow rate of the HP brine has not changed significantly, and the HP brine pressure will first fluctuate downward to adapt to this change.

3.1.2. Flow rate fluctuation of HP brine in different capacities

The flow rate curves of HP brine at various capacities are displayed in Fig. 5. The pulsation characteristics of flow rate are pretty different from pressure pulsation, showing the features of periodic upward fluctuations, and the pulsation amplitude is smaller than the pressure pulsation amplitude. With the increase of processing capacity, pulsation amplitude shows a slightly upward trend, but the overall pulsation amplitude does not change much. As shown from Fig. 6, the processing capacity varying from 10 to 16 m^3/h under the operating pressure of 5.0 MPa, the pulsation amplitude of HP brine flow rate is between 0.153 and 0.186 m^3/h. At 16 m^3/h, the flow rate pulsation amplitude dropped to 0.164 m^3/h. Under the design flow rate of 12 m^3/h, the flow rate pulsation amplitude is 0.186 m^3/h, which only occupies 1.5% of the HP brine. Compared with the flow rate pulsation amplitude of 1.22 m^3/h in SB-ERD at 22 m^3/h (5.55% pulsation ratio), flow rate pulsation ratio of MRS-ERD is 1.5%. In the case of variable capacity, the HP brine flow rate is still stable, and the entire system is well adapted to pulsating conditions caused by flow rate variation.

In SB-ERD, the flow rate fluctuation of the HP brine is determined by the switcher and the moving speed of the piston [25]. In MRS-ERD, the reason for the fluctuation of the HP brine flow rate is mainly due to the switching working state of the hydraulic actuator [31]. The influence of the hydraulic actuator on flow rate is primarily reflected in two aspects. On the one hand, the hydraulic actuator has a diversion effect on the flow rate of HP brine. Although the diversion effect of the hydraulic actuator will affect the pressure and flow rate fluctuations of the HP brine, and the fluctuation of the HP brine can compensate for the impact of the split flow rate, the compensation sequence of the two is different. When compensating the split flow rate of the hydraulic actuator, the HP brine pressure has priority over the HP brine flow rate. In the transposition of the actuator, the HP brine pressure first responds to the influence of the split flow and fluctuates downwards. When the HP brine pressure fluctuation and the fluctuation of the permeating flow rate are not enough to compensate for the effect of the split flow, the HP brine flow rate plays a compensation role. To compensate for the impact of the remaining split flow, the flow rate of HP brine should also fluctuate downward, but the amplitude of the fluctuation is smaller than the amplitude of the pressure fluctuation. On the other hand, during the switching process of the hydraulic actuator, the flow area of the flow channel is adjusted, then the pressure loss in the flow process is changed. So the pipeline characteristics are changed, and

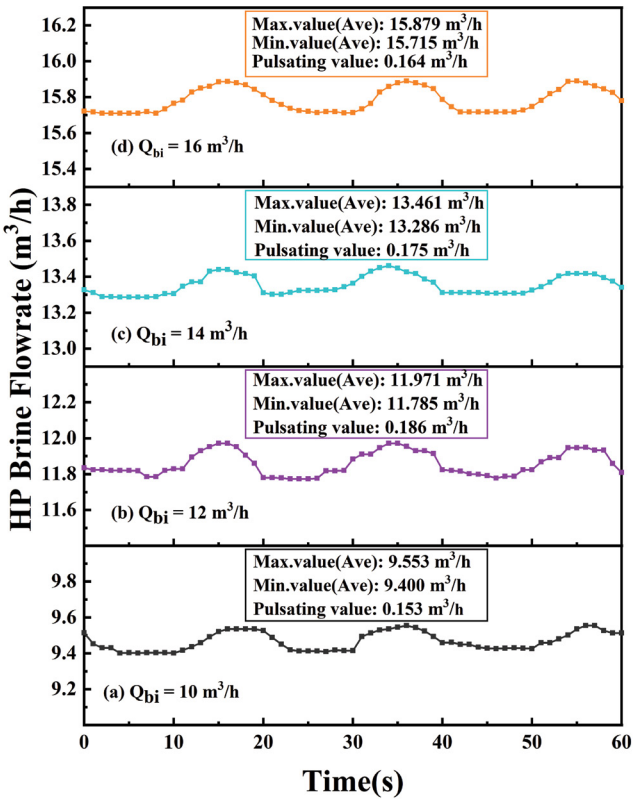

Fig. 5. Flow rate curves of HP brine at different capacities.

the working point of the booster pump is affected, which leads to a change in the flow rate of HP brine [21]. In Fig. 6 we can see that when the hydraulic actuator is switched, the pressure loss decreases, and the flow rate of the HP brine should show an upward fluctuation trend. Overall, the flow area change during the hydraulic actuator's switching process has a greater impact on the HP brine flow rate than the diversion effect, which leads to the upward fluctuation of the HP brine flow rate. The reduction in the ability of booster pump to compensate for flow rate fluctuations results in a decrease in pulsation amplitude at 14 and 16 m^3/h.

3.1.3. Pressure loss of HP brine in different capacities

The pressure loss of the HP fluid not only reflects the rationality of the device's flow channel setting but also directly affects the energy recovery efficiency of the device, which is essential to the performance evaluation of the ERD. The pressure loss of the HP fluid is collected and analyzed by setting a differential pressure transmitter between the HP brine and seawater.

Fig. 6 gives the HP brine pressure loss curve in different capacities. The HP brine pressure loss presents the characteristics of pulsing upwards first and then pulsing downwards, and the pulsation amplitude of the pressure loss increases with the increase of capacity. The smallest pulsation amplitude is 0.022 MPa, and the largest pulsation amplitude is 0.032 MPa. Under the design capacity (12 m^3/h), the maximum and minimum pressure losses are 0.094 and 0.067 MPa,

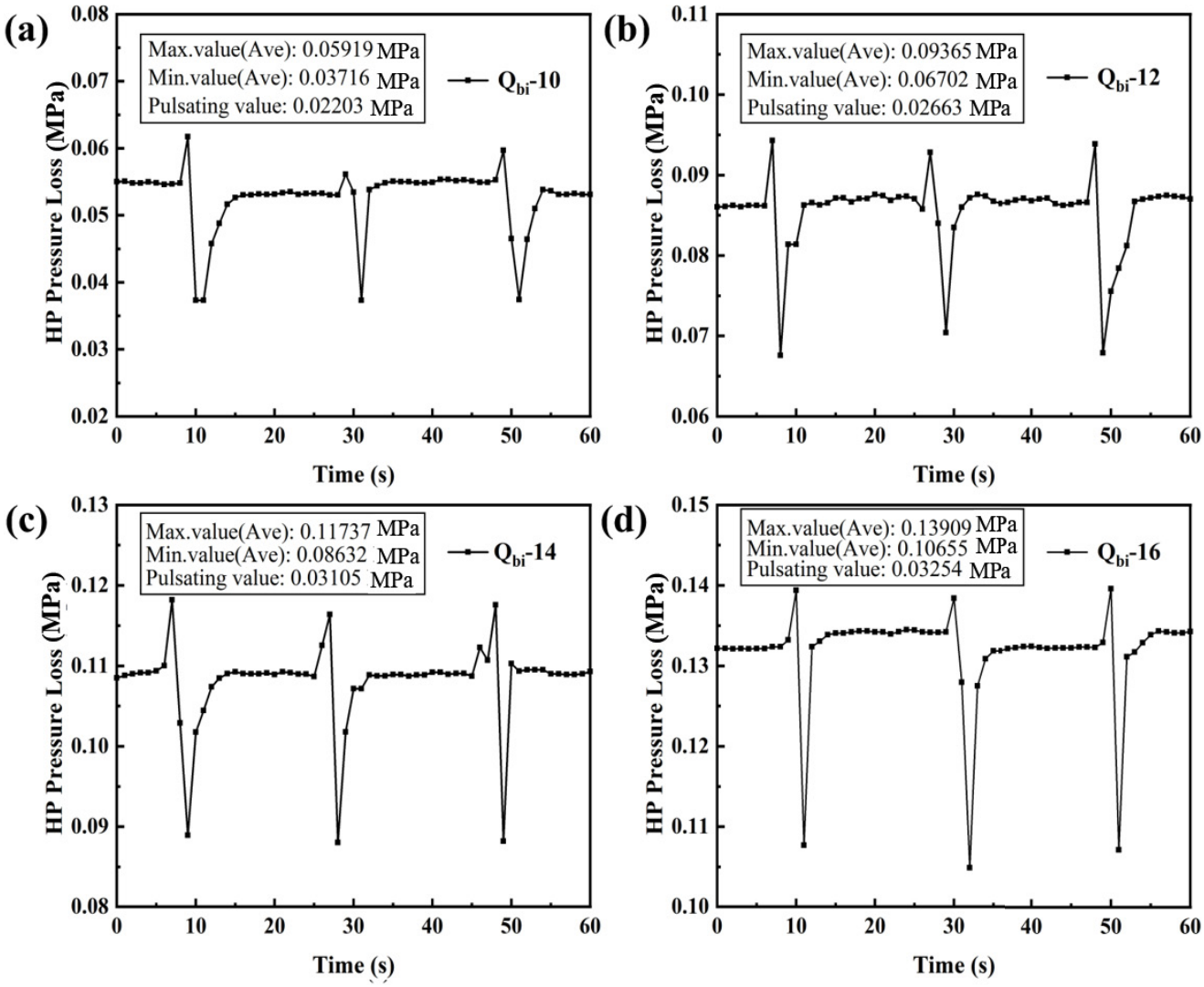

Fig. 6. Pressure loss curve of HP brine at different capacities.

respectively. The average pressure loss is 0.086 MPa, and the pulsation amplitude of pressure loss is 0.026 MPa.

Due to the HP overlap function, at the beginning of high-pressure switching, one valve plate of the hydraulic actuator is being closed, and the other valve plate is held stationary. The duration of this process is concise, less than a second. The overall opening is getting smaller, resulting in a transient increase in pressure loss. When one valve plate is closed to a certain extent, the other valve plate begins to be opened, and the entire opening of the two valve plates remains unchanged. Still, the total flow area becomes larger, and the pressure loss begins to decrease. When one valve plate is fully closed, the other is also fully opened, and the pressure loss returns to a stable state. Both pressure loss and pulsation amplitude increase slightly with the increase of capacity due to increased flow velocity. Within the capacity range from 10 to 16 m^3/h, the pressure loss and pulsation amplitude increased by 0.075 and 0.01 MPa, respectively, revealing that the MRS-ERD has good capacity flexibility and operational stability.

3.2. Fluctuation characteristics of LP fluid for MRS-ERD

Due to the low pressure of the LP fluid, it is generally believed that the LP fluid has far less influence on the stability of the entire system than the HP fluid in the stability studies of SWRO systems. However, the pulsation analysis of pressure, flow rate and pressure loss of LP fluid cannot be ignored either. In this section, we still use the pulsation amplitude to assess the operation stability of MRS-ERD. Since LP brine is directly pressurized by LP seawater, both have the same fluid characteristics. In this section, LP seawater is selected as the index for evaluating operational stability.

3.2.1. Pressure fluctuation of LP seawater in different capacities

Fig. 7 exhibits the pressure characteristic curve of LP seawater under different capacities. It can be seen from Fig. 7 that the pressure curve periodically fluctuates

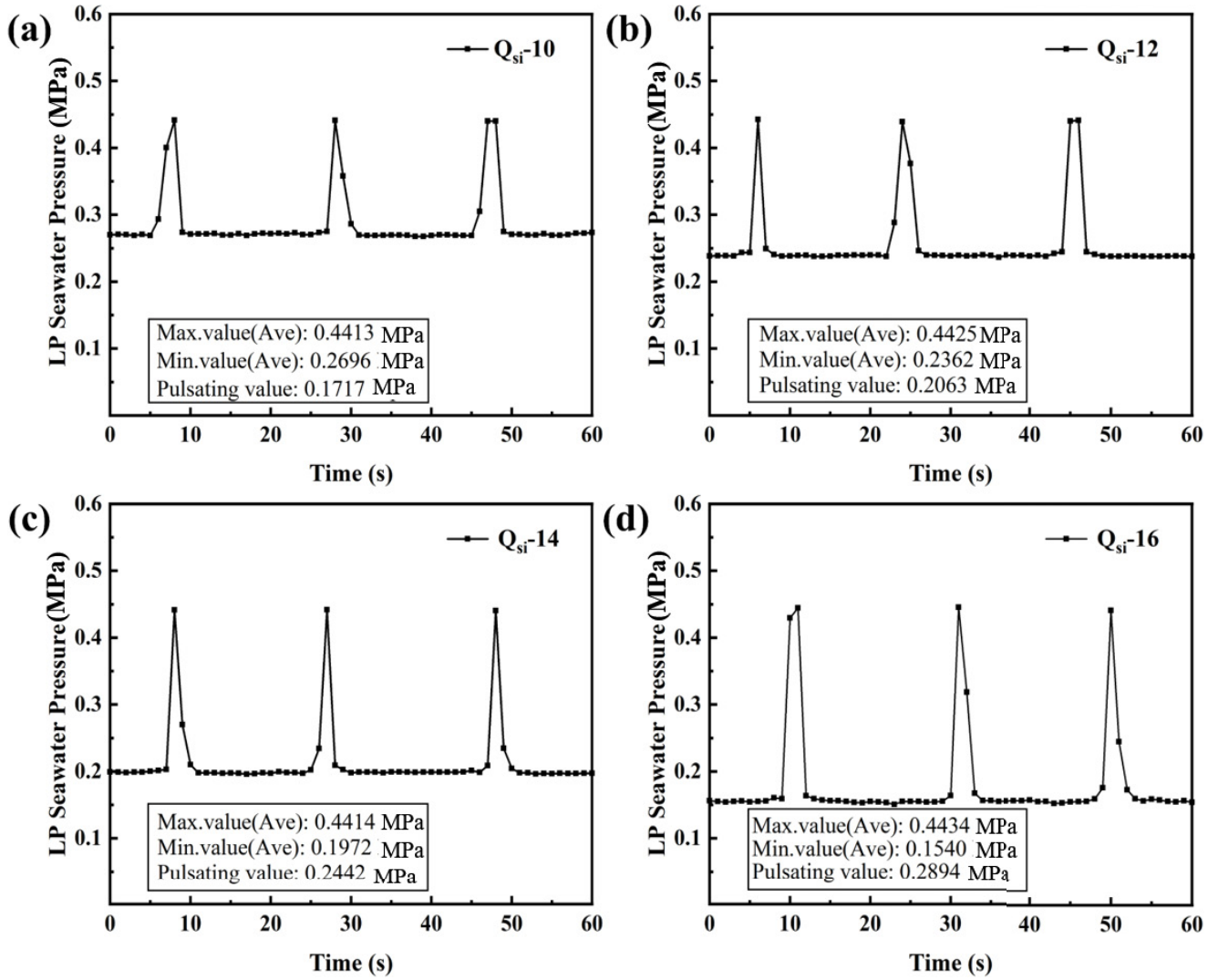

Fig. 7. Pressure curve of LP seawater at different capacities.

upward. When the capacity increases from 10 to 16 m^3/h, the LP seawater pressure decreases slightly from 0.269 to 0.154 MPa. As can be seen from Fig. 3, there is only one feed pump in the SWRO system. The flow rate of HP seawater is controlled by adjusting the frequency of the pump. The flow rate of LP seawater is controlled by a valve between the outlet of the low- pressure pipeline and the ERD. By increasing the valve opening to increase the flow rate of the LP seawater, the channel pressure loss of the LP seawater will be reduced. Since the low-pressure seawater pressure should be equal to the sum of the channel pressure loss and the outlet pressure of LP seawater, and the low-pressure pipeline outlet maintains a constant pressure, the LP seawater pressure will decrease with the increase of the LP seawater flow rate. The decreasing of pressure is independent of the ERD. The pulsation amplitude of LP seawater also changes slightly, increasing from the minimum pulsation amplitude of 0.171 to 0.289 MPa. In the hydraulic actuator of the device, a HP overlap function is provided to ensure the continuity of the HP fluid. The HP overlap function guarantees the continuity of the HP fluid. Still, it sacrifices the continuity of the LP fluid, causing the low-pressure flow channel to be closed instantaneously so that the pressure of LP seawater fluctuates upward. During operation, with the increase of the processing capacity, the flow accumulation when the low-pressure flow channel is closed increases, causing LP seawater's pressure fluctuation to increase to a certain extent. Although the LP seawater pressure fluctuates to a certain extent within the test range of the entire device, the fluctuation range and the amount of change are not extensive, which shows that the ERD has good operational stability to the LP seawater pressure.

3.2.2. Flow rate fluctuation of LP seawater in different capacities

Fig. 8 shows the flow rate curves of LP seawater under different capacities. The flow rate fluctuates downward periodically. When the capacity increases from 10 to 16 m^3/h,

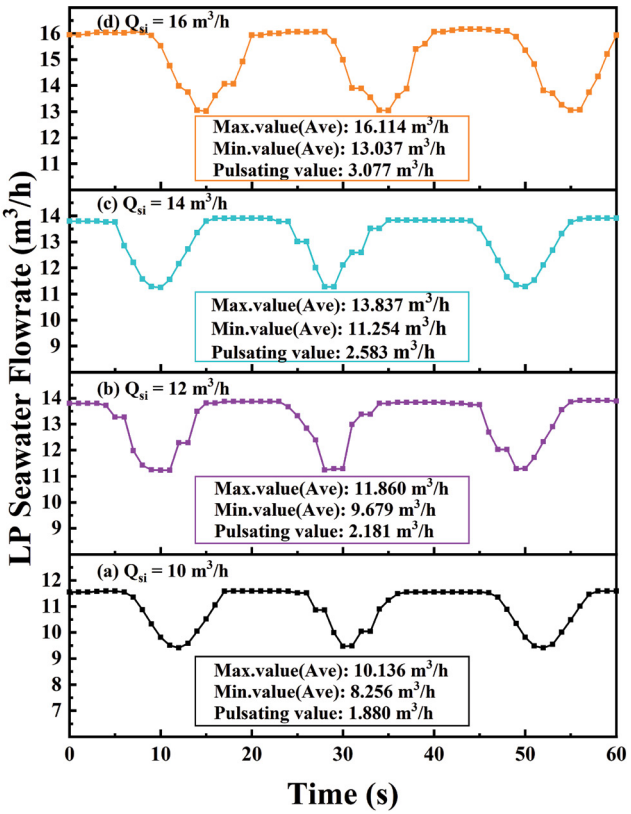

Fig. 8. Flow rate curve of LP seawater at different capacities.

the pulsation amplitude gradually increases from the minimum pulsation amplitude of 1.88 to 3.08 m³/h. Since the low-pressure channel does not have an overlapping function, the fluid switch will cause the low-pressure channel to close instantaneously at the moment of switching. The instantaneous cut-off of the low-pressure seawater flow channel causes the downward fluctuation of the LP seawater flow rate. With the increase of the processing capacity, the instantaneous closure of the low-pressure channel has an intensified impact on the low-pressure seawater flow, which in turn leads to an increase in the fluctuation range of the low-pressure seawater. It is worth noting that there is a certain regularity between the pressure curve and the flow curve in the fluctuations. The lowest point of the flow curve approximately lays behind the highest point of the pressure curve throughout the test range, which means that pressure is more sensitive to changes in the switcher.

3.2.3. Pressure loss of LP seawater in different capacities

The pressure loss of the LP fluid is directly related to the selection of the feedwater pump, and the rationality of the low-pressure flow channel is also reflected through it. The pressure loss of the LP fluid is collected and analyzed by setting a differential pressure transmitter between the LP seawater and LP brine.

Fig. 9 shows the pressure loss curve of LP seawater under different capacities. Except for periodic upward fluctuations, the pressure loss curve remained stable as a whole. As the processing capacity of MRS-ERD increases, the steady section of the LP pressure loss curve shows a slight increase, with a rise of 0.017 MPa, and the fluctuation range of pressure loss increases to a certain extent, with an increase of 0.026 MPa. As the processing capacity increases, the flow rate of the fluid increases. Obviously, the increase of the flow rate will increase the pressure loss of the flow process. The periodic upward fluctuation in pressure loss is caused by the momentary closure of the low-pressure flow channel during the switching process of the device. At the moment when the low-pressure flow channel is closed, the LP seawater is in a pressurized state, the LP brine maintains normal pressure, and there is a maximum pressure loss between the LP seawater and the LP brine. With the increase of the processing capacity, the maximum pressure difference between the LP seawater and the LP brine will gradually increase due to the influence of the flow rate, and the pressure loss pulsation amplitude will become larger.

3.3. Leakage and energy recovery efficiency of MRS-ERD

In this part, the performance of the MRS-ERD will be discussed from two aspects: the leakage situation and energy recovery efficiency under different processing capacities. These two aspects are critical to the subsequent application of the device in the desalination system.

In the seawater desalination system, the difference between the HP brine flow rate (Q_{bi}) and the LP seawater flow rate (Q_{so}) is commonly used to characterize the leakage (Q_1). The formula is as follows:

$$Q_1 = Q_{bi} - Q_{so} \tag{1}$$

However, in order to more accurately and intuitively reflect the leakage situation under different processing capacities, the leakage rate is often used to evaluate the leakage situation of the system [15]. Fig. 10 shows the leakage and leakage ratio of the ERD at different capacities. With the increase in processing capacity, the leakage volume tends to increase, but the increase is not significant. Although the leakage volume has increased, the leakage ratio under the corresponding processing volume has dropped from 2.7% to 1.3%. It shows that with the increase of the processing volume, the leakage trend of the entire device is decreasing, and the device can well adapt to the leakage problem caused by the change of the processing capacities.

Energy recovery efficiency is a central index for assessing energy recovery devices, and its calculation formula is as follows:

$$\eta = \frac{\sum(\text{Pressure} \times \text{Flow})_{out}}{\sum(\text{Pressure} \times \text{Flow})_{in}} = \frac{Q_{so} \cdot P_{so} + Q_{bo} \cdot P_{bo}}{Q_{si} \cdot P_{si} + Q_{bi} \cdot P_{bi}} \tag{2}$$

Fig. 11 shows the energy recovery efficiency curve of the ERD under different processing capacities. When processing capacity increases from 6 to 16 m³/h, energy recovery efficiency is relatively stable, always maintaining above 96.33%. The energy recovery efficiency changes in two stages. When the capacity is increased from 6 to 12 m³/h, the device efficiency rises from 96.51% to 97.45%. As the

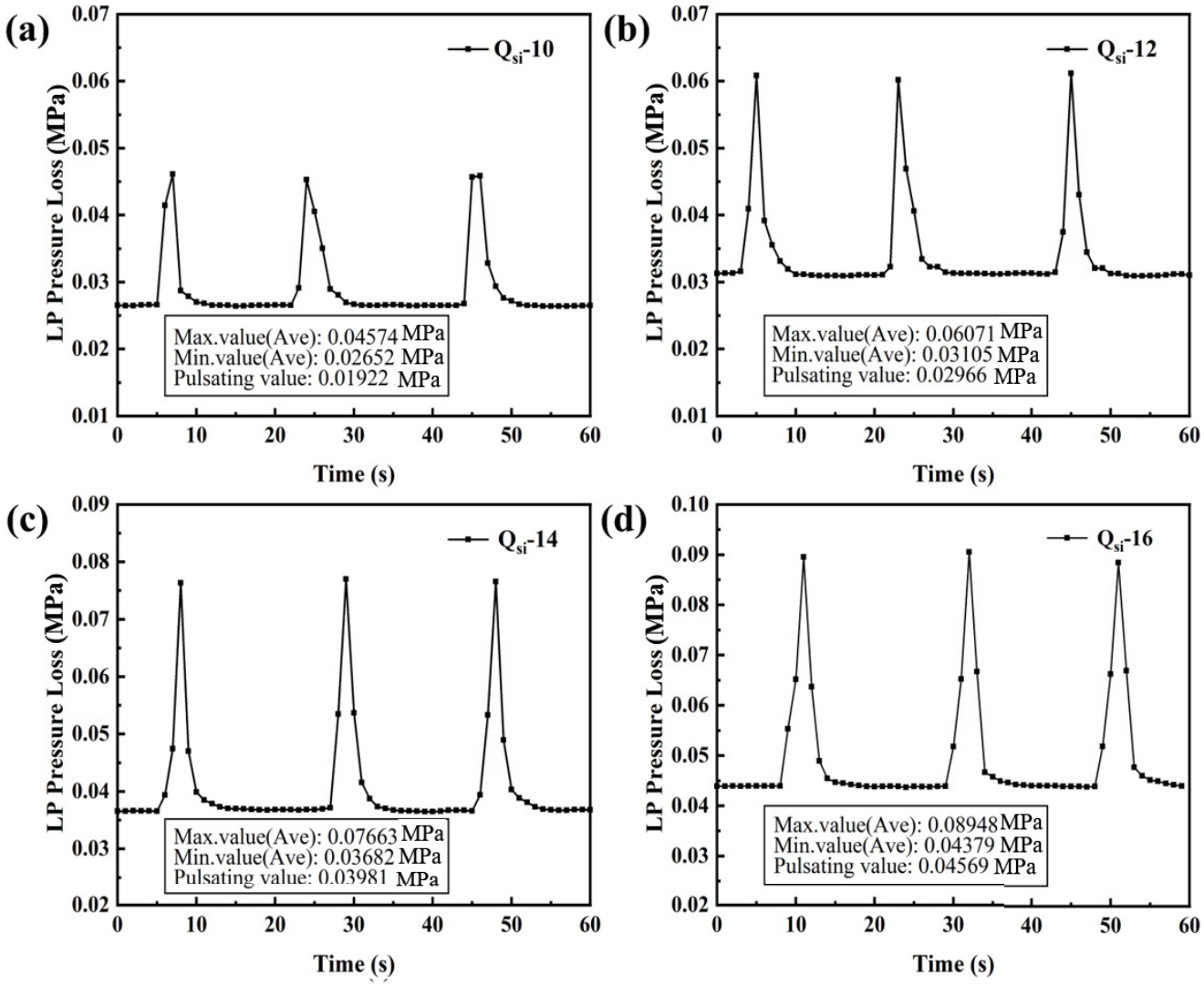

Fig. 9. Pressure loss curve of LP seawater at different capacities.

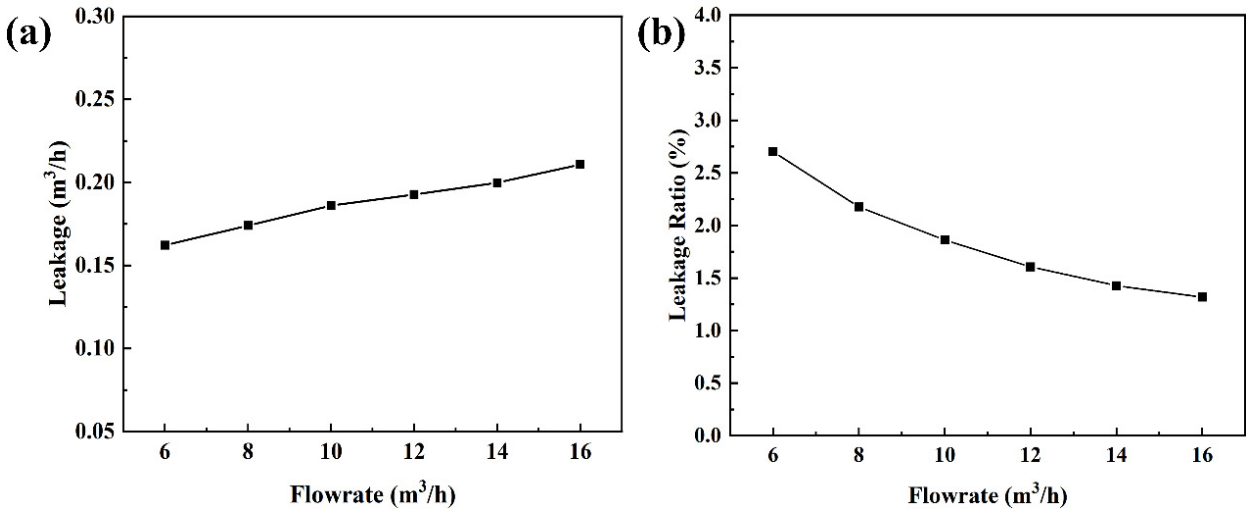

Fig. 10. Leakage and leakage ratio of the ERD at different capacities.

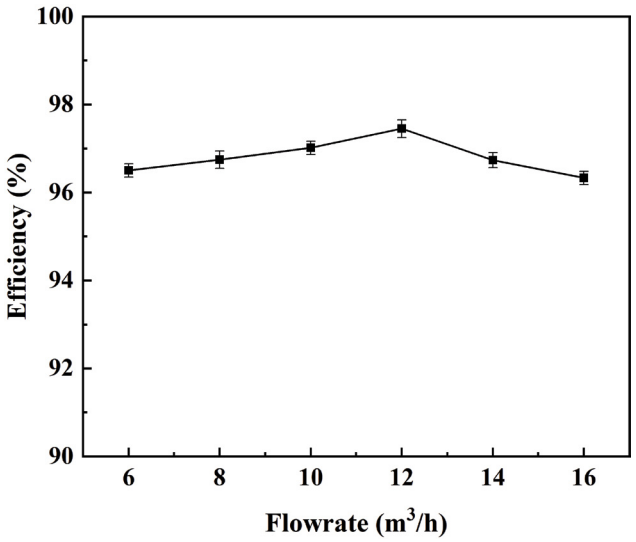

Fig. 11. Energy recovery efficiency under different capacities.

capacity is increased from 12 to 16 m³/h, the device efficiency decreases from 97.45% to 96.33%. It is because the leakage ratio of the device drops rapidly in the first stage, the pressure loss changes little, and the energy recovery efficiency of the device is improved. At this time, the leakage ratio is the main factor of efficiency. In the second-stage, pressure loss of the device increases and leakage ratio changes slowly, and the efficiency of device has a downward trend. In this stage, pressure loss is the main factor. Under different processing capacities, MRS-ERD can still have a high energy recovery efficiency, which benefits from the device's excellent sealing performance and lower pressure loss.

3.4. Energy consumption of MRS-ERD

The energy required per unit output of permeate can be expressed in terms of the specific energy, which is an important parameter of the SWRO system. The specific energy in the SWRO is defined as the following equations:

$$\mathrm{SE} = \frac{\left(E_{\mathrm{HP}} + E_{\mathrm{BP}} + E_{\mathrm{SP}}\right)}{Q_P} \tag{3}$$

where SE is the SWRO system specific energy, E_{HP} the high-pressure pump energy consumed, E_{BP} the booster pump energy consumed, E_{SP} the supply pump energy consumed, Q_P the permeate flow rate.

$$\mathrm{SE} = \frac{\left(Q_{\mathrm{HP}}\left(P_{\mathrm{HP}} - P_F\right)/\eta_{\mathrm{HP}} + Q_{\mathrm{BP}}\left(P_{\mathrm{HP}} - P_{\mathrm{BPI}}\right)/\eta_{\mathrm{BP}} + Q_{\mathrm{SP}}P_F/\eta_{\mathrm{SP}}\right)}{3.6Q_P} \tag{4}$$

where Q_{HP} the high-pressure pump flow rate, P_{HP} the high-pressure pump outlet pressure, P_F the high-pressure pump feedwater pressure, η_{HP} the high-pressure pump and motor efficiency, Q_{BP} the booster pump flow rate, P_{BPI} the booster pump inlet pressure, η_{BP} the booster pump and motor efficiency, Q_{SP} the supply pump flow rate, and η_{SP} the supply pump and motor efficiency.

In this paper, the motor efficiencies of the high-pressure pump booster pump and supply pump are 78%, 77%, and 76%, respectively. Under 5.0 MPa and the design flow rate (12 m³/h) of ERD, the permeate flow rate is 6.87 m³/h, and the specific energy consumption is 2.43 kWh/m³, which is competitive in commercial ERD.

4. Conclusions

In this work, the SB-ERD was modified to a miniaturized reciprocating-switcher energy recovery device (MRS-ERD), and an experimental platform for the SWRO system was built. The stability of the device's operation was studied from two aspects of pressure and flow rate pulsation, and its operating performances were evaluated by leakage and efficiency.

Firstly, under the operating pressure of 5.0 MPa, the capacity of the ERD varied from 10 to 16 m³/h, the pressure pulsation amplitude of HP brine was maintained at 0.20 MPa, and the pressure fluctuation amplitude of LP seawater was increased from 0.17 to 0.29 MPa. The flow rate pulsation amplitude of HP brine kept between 0.153 and 0.186 m³/h, and the flow rate fluctuation amplitude of LP seawater increased from 1.88 to 3.08 m³/h. The HP overlap function can effectively reduce the pulsation amplitude of HP fluid, but it has no noticeable effect on the pulsation amplitude of LP fluid. The pressure pulsation ratio of MRS-ERD is 4.26% at design capacity (12 m³/h), which is 2.41% lower than the SB-ERD. Compared with the flow rate pulsation amplitude of 1.22 m³/h in SB-ERD at 22 m³/h (5.55% pulsation ratio), flow rate pulsation ratio of MRS-ERD is only 1.5%. On the whole, the MRS-ERD runs stably in 80%–130% of the designed capacity and 5.0 MPa.

Secondly, the causes of pressure and flow rate fluctuations are qualitatively analyzed. The transformation of the working position of the switcher causes the change of the high and low-pressure fluid flow path. The switcher's shunting effect and the booster pump's compensation effect jointly determine the pulsation of HP fluid. The interruption of the low-pressure flow channel leads to the pulsation of LP fluid.

Thirdly, though there is a slight ascent in leakage, the leakage ratio of the ERD is reduced from 2.7% to 1.3%, and the energy recovery efficiency remains above 96.33% and the specific energy consumption is 2.43 kWh/m³ at the design flow rate (12 m³/h), which is competitive in commercial ERD.

Development and operational performance studies for MRS-ERD to satisfy small and medium-sized desalination needs are expected in future work.

Symbols

P_{bi}	—	Pressure of HP brine inlet, MPa
P_{si}	—	Pressure of LP seawater inlet, MPa
Q_{bi}	—	Flow rate of HP brine inlet, m³/h
Q_{si}	—	Flow rate of LP seawater inlet, m³/h
P_{bo}	—	Pressure of LP brine outlet, MPa
P_{so}	—	Pressure of HP seawater outlet, MPa

Q_{bo} — Flow rate of LP brine outlet, m^3/h
Q_{so} — Flow rate of HP seawater outlet, m^3/h
Q_1 — Leakage flow rate, m^3/h
η — Energy recovery efficiency, %
SE — Specific energy, kWh/h^3
E_{HP} — High-pressure pump energy consumed, kW
E_{BP} — Booster pump energy consumed, kW
E_{SP} — Supply pump energy consumed, kW
Q_P — Permeate flow rate, m^3/h
Q_{HP} — High-pressure pump flow rate, m^3/h
Q_{BP} — Booster pump flow rate, m^3/h
Q_{SP} — Supply pump flow rate, m^3/h
P_{HP} — High-pressure pump outlet pressure, MPa
P_F — High-pressure pump feedwater pressure, MPa
P_{BPI} — Booster pump inlet pressure, MPa
η_{HP} — High-pressure pump and motor efficiency, %
η_{BP} — Booster pump and motor efficiency, %
η_{SP} — Supply pump and motor efficiency, %

Acknowledgments

This research is supported by the National Key Research and Development Program of China (2017YFC0403800) and the State Key Laboratory of Chemical Engineering (SKL-ChE-17T02).

References

[1] R. Wang, J. Zimmerman, Hybrid analysis of blue water consumption and water scarcity implications at the global, national, and basin levels in an increasingly globalized world, Environ. Sci. Technol., 50 (2016) 5143–5153.
[2] M. Elimelech, W.A. Phillip, The future of seawater desalination: energy, technology, and the environment, Science, 333 (2011) 712–717.
[3] G. Meerganz von Medeazza, V. Moreau, Modelling of water–energy systems. The case of desalination, Energy, 32 (2007) 1024–1031.
[4] J. Song, T. Li, L. Wright-Contreras, A.W.-K. Law, A review of the current status of small-scale seawater reverse osmosis desalination, Water Int., 42 (2017) 618–631.
[5] A. Subramani, M. Badruzzaman, J. Oppenheimer, J.G. Jacangelo, Energy minimization strategies and renewable energy utilization for desalination: a review, Water Res., 45 (2011) 1907–1920.
[6] M. Thomson, M.S. Miranda, D. Infield, A small-scale seawater reverse-osmosis system with excellent energy efficiency over a wide operating range, Desalination, 153 (2002) 229–236.
[7] V.G. Gude, Energy consumption and recovery in reverse osmosis, Desal. Water Treat., 36 (2012) 239–260.
[8] J. Kim, K. Park, D.R. Yang, S. Hong, A comprehensive review of energy consumption of seawater reverse osmosis desalination plants, Appl. Energy, 254 (2019) 113652, doi: 10.1016/j.apenergy.2019.113652.
[9] S. Bross, W. Kochanowski, N. El Maraghy, SWRO-core-hydraulic-system: first field test experience, Desalination, 184 (2005) 223–232.
[10] C.C. Mei, Y.-H. Liu, A.W.K. Law, Theory of isobaric pressure exchanger for desalination, Desal. Water Treat., 39 (2012) 112–122.
[11] P.D. Richard L. Stover, Development of a fourth generation energy recovery device, Desalination, 165 (2004) 313–321.
[12] R.L. Stover, Seawater reverse osmosis with isobaric energy recovery devices, Desalination, 203 (2007) 168–175.
[13] R.L. Stover, B. Andrews, Isobaric energy-recovery devices: past, present, and future, IDA J. Desal. Water Reuse, 4 (2013) 38–43.
[14] I.B. Cameron, R.B. Clemente, SWRO with ERI's PX pressure exchanger device — a global survey, Desalination, 221 (2008) 136–142.
[15] N. Liu, Z. Liu, Y. Li, L. Sang, An optimization study on the seal structure of fully-rotary valve energy recovery device by CFD, Desalination, 459 (2019) 46–58.
[16] D. Song, Y. Wang, S. Xu, J. Gao, Y. Ren, S. Wang, Analysis, experiment and application of a power-saving actuator applied in the piston type energy recovery device, Desalination, 361 (2015) 65–71.
[17] D. Song, Y. Zhang, H. Wang, L. Jiang, C. Wang, S. Wang, Z. Jiang, H. Li, Demonstration of a piston type integrated high pressure pump-energy recovery device for reverse osmosis desalination system, Desalination, 507 (2021) 115033, doi: 10.1016/j.desal.2021.115033.
[18] Y. Wang, Y. Ren, J. Zhou, E. Xu, S. Xu, Functionality test of an innovative single-cylinder energy recovery device for SWRO desalination system, Desalination, 388 (2016) 22–28.
[19] Y. Wang, S. Wang, S. Xu, Investigations on characteristics and efficiency of a positive displacement energy recovery unit, Desalination, 177 (2005) 179–185.
[20] J. Zhou, Y. Wang, Y. Duan, J. Tian, S. Xu, Capacity flexibility evaluation of a reciprocating-switcher energy recovery device for SWRO desalination system, Desalination, 416 (2017) 45–53.
[21] Z. Sun, Y. Wang, J. Zhou, Z. Xu, S. Xu, Development and operational stability evaluation of new three-cylinder energy recovery device for SWRO desalination system, Desalination, 502 (2021) 114909, doi: 10.1016/j.desal.2020.114909.
[22] N. Lasse, W.G.W. Langmaack, iSave the Easiest and Most Compact Way to Save Energy on SWRO Plants, 2010 Asia-Pacific Conference on Desalination and Water Reclamation, 2010.
[23] S.P. Center, Compact high energy system for RO plant, World Pumps, 2013 (2013) 27–28.
[24] B. Peñate, L. García-Rodríguez, Energy optimisation of existing SWRO (seawater reverse osmosis) plants with ERT (energy recovery turbines): technical and thermoeconomic assessment, Energy, 36 (2011) 613–626.
[25] J. Tian, Y. Wang, J. Zhou, Z. He, S. Xu, Development and experimental evaluation of an innovative self-boosting energy recovery device for small-scale SWRO system, Desal. Water Treat., 181 (2020) 28–37.
[26] A. Alhathal Alanezi, A. Altaee, A.O. Sharif, The effect of energy recovery device and feed flow rate on the energy efficiency of reverse osmosis process, Chem. Eng. Res. Des., 158 (2020) 12–23.
[27] S. Mambretti, E. Orsi, S. Gagliardi, R. Stover, Behaviour of energy recovery devices in unsteady flow conditions and application in the modelling of the Hamma desalination plant, Desalination, 238 (2009) 233–245.
[28] G.M. Geise, H.-S. Lee, D.J. Miller, B.D. Freeman, J.E. McGrath, D.R. Paul, Water purification by membranes: the role of polymer science, J. Polym. Sci. Pol. Phys., 48 (2010) 1685–1718.
[29] P.S. Goh, T. Matsuura, A.F. Ismail, N. Hilal, Recent trends in membranes and membrane processes for desalination, Desalination, 391 (2016) 43–60.
[30] K. Jeong, Y.G. Lee, S.J. Ki, J.H. Kim, Modeling seawater reverse osmosis system under degradation conditions of membrane performance: assessment of isobaric energy recovery devices and feed pressure control benefits, Desal. Water Treat., 57 (2015) 20210–20218.
[31] J. Zhou, Y. Wang, Z. Sun, S. Xu, Experimental and numerical investigations of overlapping function in enhancing flow continuity for reciprocating-switcher energy recovery device, Desalination, 487 (2020) 114494, doi: 10.1016/j.desal.2020.114494.
[32] J. Zhou, Y. Wang, Z. Feng, Z. He, S. Xu, Effective modifications of reciprocating-switcher energy recovery device by adopting pilot valve plates to decrease the switching load and fluid fluctuations, Desalination, 462 (2019) 39–47.

Supplementary information

Fig. S1. Field diagram of the SWRO system equipped with MRS-ERD.

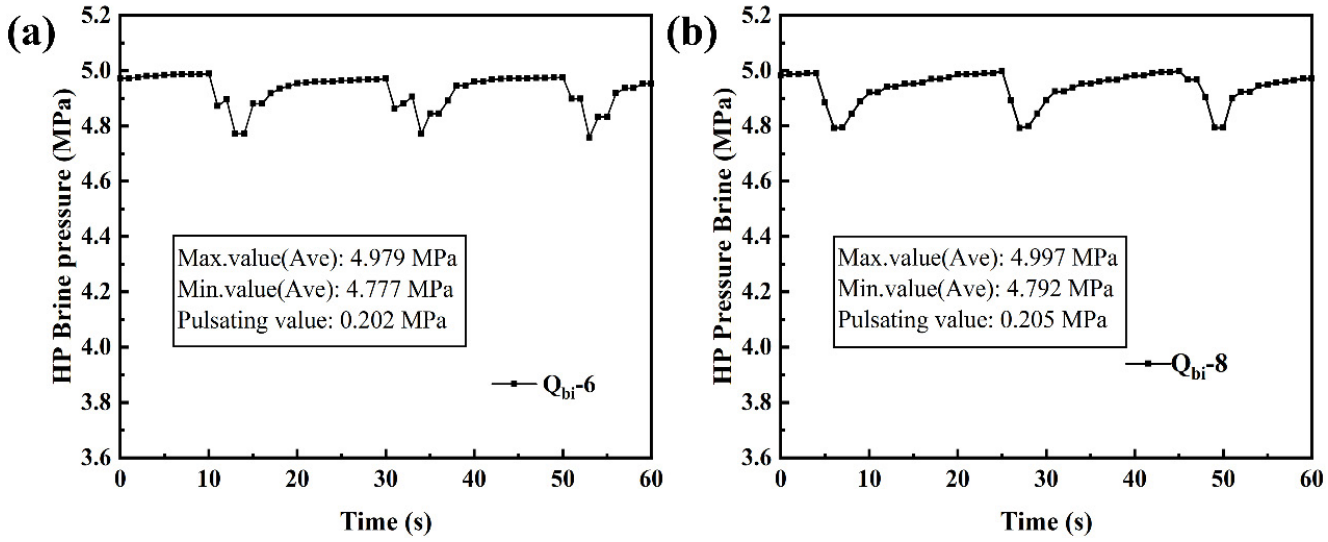

Fig. S2. Pressure curve of the HP brine at (a) 6 m^3/h and (b) 8 m^3/h.

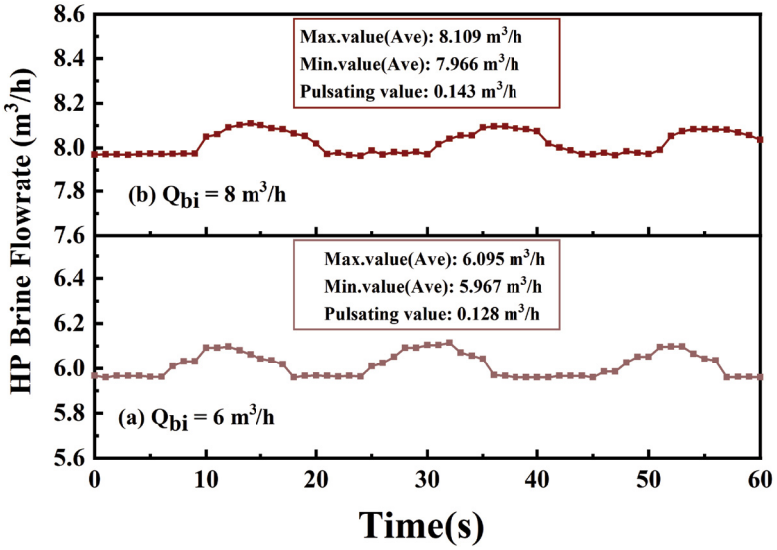

Fig. S3. Flow rate curves of HP brine at (a) 6 m³/h and (b) 8 m³/h.

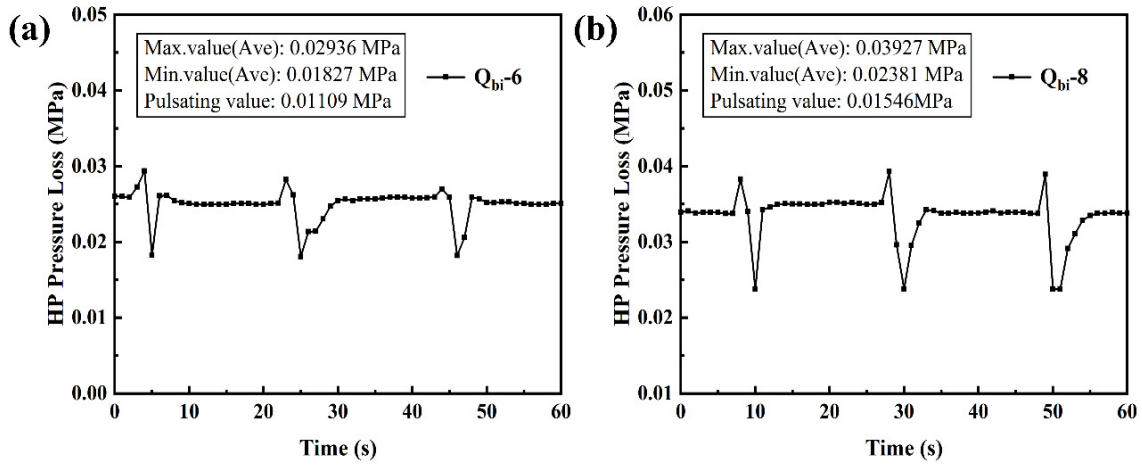

Fig. S4. Pressure loss curve of HP brine at (a) 6 m³/h and (b) 8 m³/h.

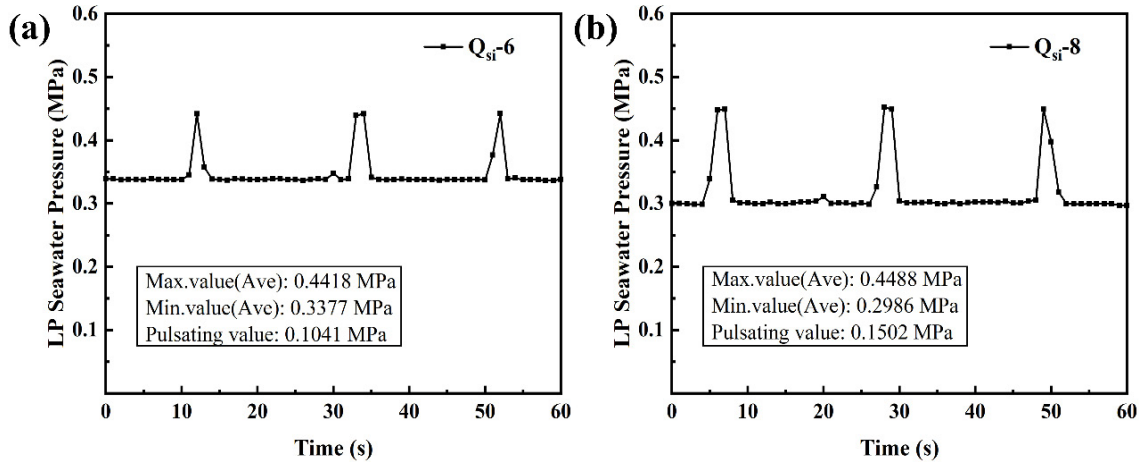

Fig. S5. Pressure curve of LP seawater at (a) 6 m³/h and (b) 8 m³/h.

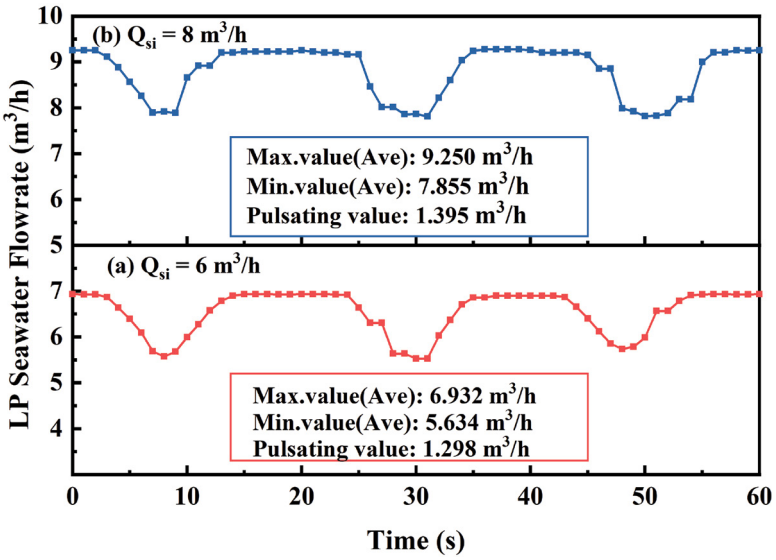

Fig. S6. Flow rate curve of LP seawater at (a) 6 m³/h and (b) 8 m³/h.

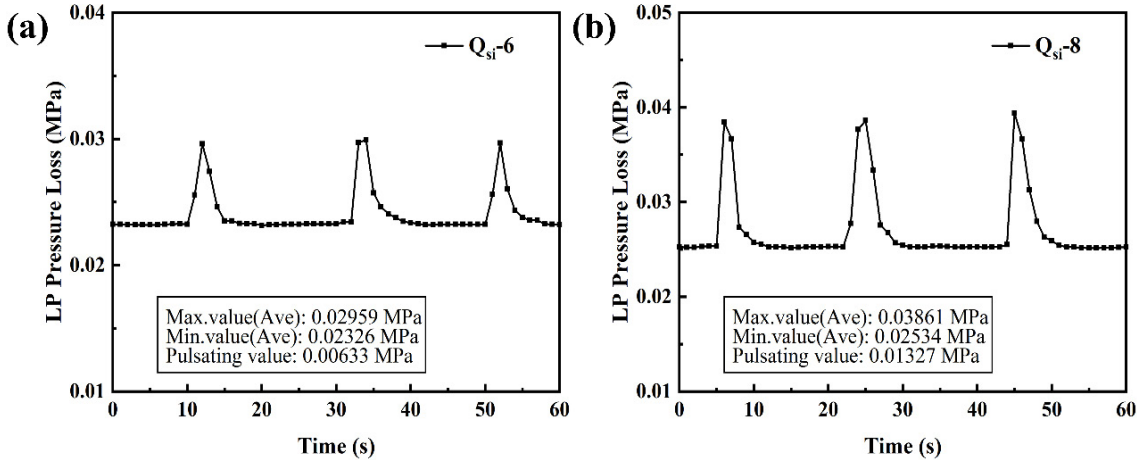

Fig. S7. Pressure loss curve of LP seawater at (a) 6 m³/h and (b) 8 m³/h.